Journal of Magnetic Resonance **156,** 242–248 (2002)
doi:10.1006/jmre.2002.2561

Resin Dynamics Contributes to the NMR Line Broadening of Organic Molecules Grafted onto a Polystyrene Resin

Guy Lippens,[1] Gianni Chessari, and Jean-Michel Wieruszeski

CNRS, Université de Lille 2 UMR 8525, Institut Pasteur de Lille and Institut de Biologie de Lille, 1 rue du Professeur Calmette, BP447, 59019 Lille Cedex, France

Received November 20, 2001; revised May 1, 2002

Despite the use of high resolution magic angle spinning NMR, the NMR linewidth of anchored molecules on the commonly used Merrifield solid phase resins remains larger than that of the corresponding molecules in solution. We investigate the different mechanisms that might be at the origin of this line broadening. Experimentally, we use the CPMG method to determine the ^{15}N relaxation times of a tethered tripeptide and show that the slow resin dynamics significantly contributes to the transverse relaxation. © 2002 Elsevier Science (USA)

Key Words: **HRMAS NMR; solid phase resins; linewidth; magnetic susceptibility.**

INTRODUCTION

High resolution magic angle spinning (HR MAS) NMR is emerging as a powerful analytical tool in solid phase chemistry, as the combined swelling of the resin and spinning of the sample at the magic angle lead to spectra that are of sufficient quality to detect, identify, and even quantify most reasonably sized organic entities without the need to cleave them from the support (*1–5*). The good swelling was recognized very early on as a prerequisite for obtaining solution-like spectra (*4, 6*), but recently, several groups have pinpointed the influence of the resin itself on the quality of the NMR spectra (*7–9*). However, the exact reasons why one observes larger linewidths than in solution upon using the classical Merrifield resin or related resins, built from a slightly cross-linked polystyrene backbone, still are not clear. The aim of the present paper is to investigate the different factors that might contribute and give both theoretical and experimental evidence that the aromatic nature of the resin combined with its dynamics rather than the dynamics of the peptide alone is at the origin of the phenomenon.

MATERIAL AND METHODS

Sample preparation. ^{15}N-labeled Ala and Gly residues were purchased from Cambridge Isotope Laboratories. The Phe sample, labeled at the level of 34%, was a generous gift from Dr. O. Barzu (Paris, France). The peptide Ala-Phe-Gly (**1**) was synthesized using the Fmoc strategy on 150 mg (0.29 mmol) of *p*-aminomethyl-polystyrene resin (LCC-Dynospheres), carrying a nominal charge of 1.95 mmol/g. After the synthesis the resin was treated with a solution of 20% TFA in dichloromethane (DCM) for 10 min and then washed extensively with DCM and dried under vacuum conditions for one day. This procedure allowed us to have the N terminal Ala residue of the peptide in the protonated form with trifluoroacetate as counterion. The resin sample was prepared by introducing 10 mg of dry Dynospheres into a full rotor (100-μl volume) and by *in situ* swelling with deuterated DMF.

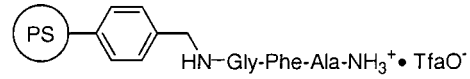

1-TFA

NMR spectroscopy. NMR experiments were recorded on a Bruker DMX 600-MHz spectrometer, equipped with a triple resonance HRMAS probe with uni-axial pulsed field gradients. A spinning rate of 6 kHz was consistently used throughout the study. ^{15}N spectra were recorded in the direct mode, with 4k complex points in the acquisition and with a recycle delay of 5 s. Typically, 4096 scans per increment were recorded for the heteronuclear NOE measurements, and 1024 for the T_2 experiments. Heteronuclear NOE values were extracted from the ^{15}N single pulse experiment with and without proton decoupling (Waltz16 decoupling, with a 2.1-kHz proton $\mathbf{B}_1$ field, centered on the amide protons) during the 5-s recycle delay. The T_2 CPMG series was performed starting directly from nitrogen magnetization followed by a CPMG pulse train (*10, 11*). The initial CPMG measurements were performed with a 333-μs delay separating the centers of the 26-μs ^{15}N π-pulses, corresponding to one π-pulse per two rotor periods. CPMG pulse trains were 1.3-, 10.7-, 30.7-, 60-, 100-, 200-, and 300-ms long and were implemented as an integer number of the rotor period in order to avoid problems with $\mathbf{B}_1$ inhomogeneities (*12–14*). Care was taken to remove any cross-correlation effects by proton decoupling during the CPMG train (*15*). In order to investigate the contribution

[1] To whom correspondence should be addressed.

1090-7807/02 $35.00

TABLE 1
Values for the Correlation Time Derived from the NOE Effect and Used to Derive Theoretical T_2 Values

Residue	Gly	Phe	Ala
Exp NOE effect η	−1.73	−2.09	−4.58
Deduced τ_c	0.8 ns	0.7 ns	0.9 ns
Theoretical T_2	444 ms	486 ms	409 ms
Exp linewidth $\Delta\nu$	21 Hz	12 Hz	7 Hz
Deduced T_2	15 ms	26 ms	45 ms
T_2 exp($\delta = 667$ μs)	73 ms	83 ms	69 ms
T_2 exp($\delta = 333$ μs)	121 ms	197 ms	101 ms
T_2 exp($\delta = 166$ μs)	125 ms	229 ms	221 ms
T_2 exp($\delta = 83$ μs)	184 ms	434 ms	426 ms

Note. For the ammonium moiety, we neglected any cross-correlation effects and simply considered that the NOE enhancement comes from three independent protons. The T_2 times derived from the linewidth $\Delta\nu$ were calculated as $T_2 = 1/(\pi\Delta\nu)$.

of chemical exchange to the T_2 relaxation, several additional series with different δ delays between the π-pulses were recorded. Series with $\delta = 83.3$, 166.7, and 666.7 μs correspond to two or one π-pulses per rotor period, or one π-pulse every four rotor periods.

All data were transformed after multiplication with an exponential window to 8k complex points. Integrals were defined within the SNARF program (F. Van Hoesel, Groningen, the Netherlands). Heteronuclear enhancement factors were derived form the ratio f between the nondecoupled and the decoupled spectra as $\eta = 1/f - 1$. Relaxation data were fitted to an exponential decaying function by a least square procedure, and the decay rate was interpreted as the T_2 time.

Theoretical interpretation of the relaxation rates. Assuming the relaxation to be mainly of dipolar origin, accompanied by a contribution of the chemical shift anisotropy, and following the notation of Ref. (*16*), the relaxation parameters were interpreted as a function of spectral density functions with the analytical form $J(\omega) = 2/15\tau_c/(1 + \omega^2\tau_c^2)$, where τ_c is the correlation time describing the decay of the dipolar interaction. As we regard the relaxation parameters on a per-residue basis, no effort was made to distinguish overall and internal movements with the accompanying order factor. We used a value of 1.02 Å for r_{NH} and a value of 160 ppm for the nitrogen chemical shift anisotropy (*17*) in order to obtain the theoretical T_2 values listed in Table 1. The contribution Δ_{ex} to the T_2 relaxation rate for a two-site chemical exchange process with rate constant k_{ex} as a function of delay δ between the π-pulses in the CPMG train was modeled according to (*25*) as

$$\Delta_{ex} = 1/4(k_{ex} - 1/(2\delta)\sinh^{-1}(\delta k_{ex}\sinh(2u)/u))$$

with

$$u = \delta\sqrt{k_{ex}^2 - \Omega_{ex}^2}$$

and Ω_{ex} the difference in radial frequency for the given nucleus in both sites.

RESULTS

The 1D proton spectrum of the resin shows three resonances in the amide proton region, corresponding to the three amino acids in the Gly-Phe-Ala peptide coupled to the resin. One of the lines is broader than the two others and was assigned by exchange spectroscopy to the protons of the N-terminal NH_3^+ moiety, which is broadened due to exchange with the residual water (*18*). A TOCSY spectrum allowed the assignment of the three lines to the Phe amide at 8.89 ppm, the Gly amide at 8.46 ppm, and the Ala NH_3^+ moiety at 8.64 ppm. The nitrogen spectrum confirms the presence of three ^{15}N nuclei and was assigned through a HSQC spectrum correlating proton and nitrogen resonances (Fig. 1). The resulting nitrogen lines at 131.5 ppm for the Phe residue, 120.0 ppm for the Gly closest to the resin, and 54.0 ppm for the ammonium group of the Ala residue are characterized by different linewidths. We found 21 Hz for Gly, 12 Hz for Phe, and 7 Hz for the Ala nitrogen line.

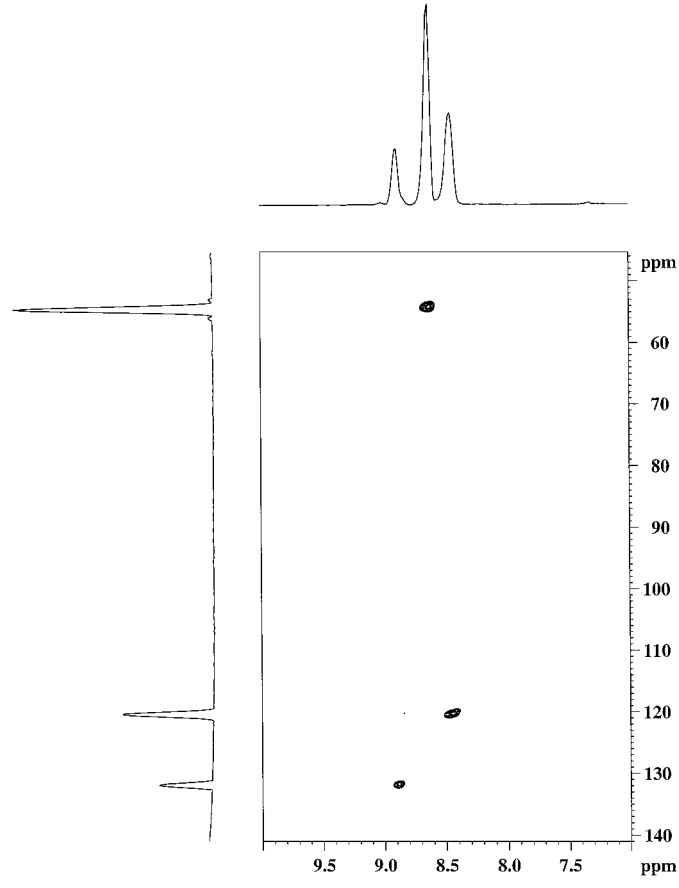

FIG. 1. ^{1}H–^{15}N HSQC spectrum of the peptidyl resin. Projections are the proton (horizontal) and the nitrogen (vertical) 1D spectra. The intensity of the Phe nitrogen signal is weaker due to the partial labeling of the amino acid.

In order to characterize the dynamics of the peptide, we recorded two nitrogen spectra with and without proton decoupling during the 5-s recycle delay. The effect of the proton decoupling indeed was dramatic, as proton decoupling not only led to a sign inversion of the lines but equally to a twofold increase of the signal intensity for the two amide nitrogens (Fig. 2). As the NOE enhancement can be interpreted as the ratio between a cross- and auto-relaxation rate, its analytical form does not depend on any order parameter, and its value can therefore be used to extract a correlation time for the dipolar interaction between the nitrogen and its directly attached proton(s) (*19–21*). Using the classical form of the NOE enhancement as a function of the appropriate spectral densities assuming dipolar and CSA mediated relaxation for the nitrogen spin (*19*), we found values slightly inferior to 1 ns for all three groups (Table 1).

Whereas this value correctly predicts the presence of negative proton–proton NOE effects (for protons, $\omega_H \tau_c > 1$ when $\tau_c \cong$ 1 ns) that we and others have observed (*8, 22, 23*), it does not explain the experimentally determined linewidths. Indeed, using the same spectral density functions in the expression for the T_2 relaxation times, a value of τ_c slightly inferior to 1 ns leads to relaxation times of 400–500 ms and therefore to linewidths inferior to 1 Hz (Table 1). Because the linewidth measured as the full width at half maximum cannot sort out true dipolar relaxation from a potential static or dynamic distribution of chemical shift values due to instrumental imperfections or sample heterogeneity, we decided to use the CPMG method to obtain an independent measure of the relaxation properties. The π-pulses used in this experiment, next to refocusing the instrumental imperfections (traditionally indicated by the T_2^* relaxation time), should refocus the broadening that finds its origin in a static distribution of resonance frequencies inherent to the heterogeneous resin sample. A different process, linked to slow dynamics that equally influences the chemical shift, has been included as an exchange term in the expression for the T_2 relaxation rates (*24*). This term, however, can be refocused by the CPMG pulse train at the condition that the π-pulses are separated by a time interval δ inferior to the time scale that characterizes the chemical exchange process (*25–27*). We therefore implemented the CPMG-based T_2 relaxation measurements with shorter delays between the π-pulses and noticed indeed that the transverse magnetization decayed significantly less upon increasing the effective $\mathbf{B}_1$ field (Fig. 3). This directly leads to increased relaxation times, especially for the two nitrogens carried by the residues that are not directly attached to the resin (Table 1).

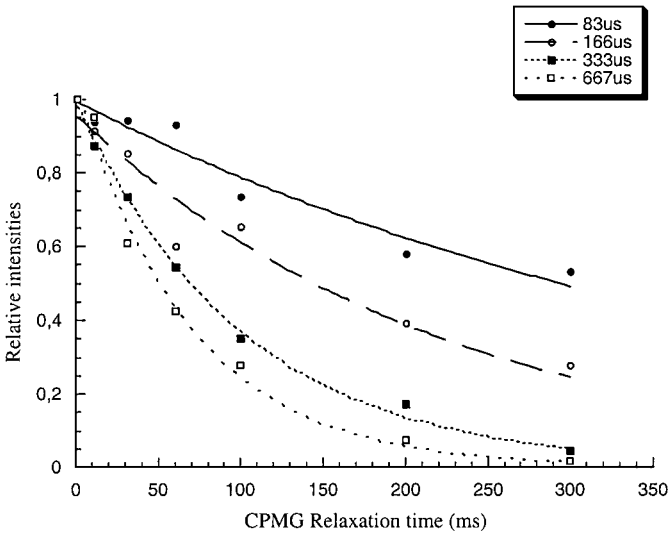

FIG. 3. Relaxation curves for the Ala nitrogen as a function of the delay δ between the π-pluses in the CPMG train. Values of δ are 83 μs (filled spheres), 166 μs (open spheres), 333 μs (filled squares) and 667 μs (open squares). The curves indicate the best exponential fit through the experimental data points.

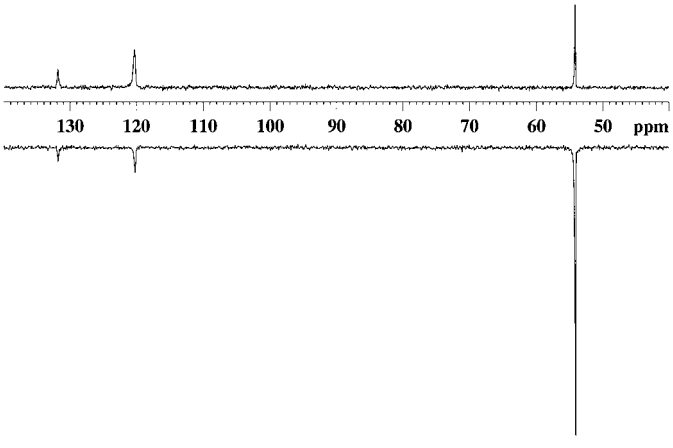

FIG. 2. Nitrogen spectra of the peptidyl resin recorded without (top) and with (bottom) proton decoupling that served for the determination of the heteronuclear NOE effect.

DISCUSSION

Whereas the above described results indicate the experimental time scales that govern the dynamics of the peptide on the resin, it still is not straightforward to interpret them in terms of microscopic behavior of the individual chain. The following discussion therefore aims to investigate the different scenarios that have been proposed in the literature as a potential source of line broadening and to reconcile our new experimental data with the observed important linewidths.

1. *Residual anisotropic interactions.* Because the peptide chains are tethered to the polystyrene backbone through a linker, one expects that a particular nucleus will not sample the complete solid angle. If hindrance comes mainly from the side where the peptide is attached, the excluded volume should be larger for those functions that are closer to the cross-linked polymer. The resulting lack of averaging of the different anisotropic interactions that dominate the NMR behavior, such as the dipolar interaction or chemical shift anisotropy, contributes to the

observed static linewidth of a couple of hundred hertz for the peptide resonances. Formally, however, it can still be described by a second order tensor, although with a reduced amplitude. Magic angle spinning therefore should get rid of it, at least when the spinning speed exceeds this static linewidth. The observation that spinning faster does not lead to further line narrowing (*23*) confirms that the origin of line broadening of the attached molecules should not be sought from the side of the residual anisotropic interactions. For the resin itself, one does observe a further narrowing of the aromatic resonances upon faster spinning, and residual couplings that exceed the commonly used spinning rates ($<$10 kHz) certainly contribute to the broadening of the resin signals.

2. *Rotational dynamics of the peptide.* The dynamics of the peptide might be a second reason for the larger linewidth. Indeed, because the solvent in this heterogeneous system is the solvated resin itself (*28*), one might expect viscosity effects to play some role in the peptide dynamics. As NMR is very suitable for dynamics measurements (*29*), several authors have examined the relaxation behavior of tethered peptides. In an early study on a solvated resin without spinning, it was found that the T_1 times for Cα nuclei of a tethered peptide were comparable to those for small free peptides in solution, despite the large difference in linewidth (*30*). The authors deduced that a linear chain attached to a polymer shows a high degree of mobility, which is of considerable interest for the chemistry on the beads. Later, NMR relaxation times were used to evaluate the mobility of a tripeptide on different polymer supports, and from the increased T_1 times when using a flexible polyoxethylene linker between the polystyrene backbone and the peptide, it was concluded that peptides terminally bound to POE-PS grafted copolymers behave more like the homogeneous soluble POE-peptides (*31*). Very recently then, the dynamics of the tethered molecules was investigated by HR MAS NMR relaxation measurements, and ^{13}C T_1 times compatible with the earlier observations without spinning were found (*32*). We measured here the ^{15}N NOE effect for the three backbone nitrogens of a tethered tripeptide and found a value close to 1 ns for the rotational correlation time. Whereas this is slower than what would be expected for a similar small peptide in solution, it still indicates that the dynamics of the attached molecule is not sufficiently influenced by the resin attachment to explain the observed line broadening.

3. *Anisotropic bulk magnetic susceptibility (ABMS)* (*33*) is a notion that was recently invoked to describe the line broadening (*32*). The meaning of BMS is inherently macroscopic, as it translates a magnetic field into an induced magnetic moment, where both are macroscopic quantities. In systems with macroscopic order, such as crystals or layered systems, that contain molecules with an intrinsic anisotropy such as aromatic rings, the induced magnetic moment will be different when all ring planes are parallel or perpendicular to the magnetic field. For excatly the same reasons that isotropic tumbling of a protein molecule does not annihilate the ring current shift, MAS cannot average this term out to zero. A polystyrene bead, however, has no long range order that would justify its description in terms of ABMS, and rotating an individual bead in the magnetic field should not lead to a different induced magnetic moment. Assigning the source of residual line broadening to ABMS therefore clearly needs further clarification.

4. *Ring current shifts.* The observation that the nature of the solid support influences the NMR characteristics of the attached molecules, with far superior linewidths being obtained on a polyethylene based support such as POEPOP (*7–9*) compared to the PS resins, clearly suggest that the styrene moieties with their aromatic ring somehow interfere with the linewidth. Underlying the familiar ring current shift in a protein (*34*) is the fact that a random proton in the neighborhood of an aromatic ring will experience a down- or upfield shift, due to the local magnetic field generated by the ring electrons. Both semiclassical (*35*) and quantum mechanical (*36*) calculations showed that this field can be modeled as originating from a dipole, if the proton under consideration is reasonably far from the ring system. This dipolar field is not averaged out to zero by the rapid isotropic motion of the protein molecule because the dipole moment associated with the aromatic ring is not constant, but depends on the orientation of the ring normal with respect to $\mathbf{B}_0$ (*33, 37, 38*). The resulting average field leads to differential chemical shift values and is one of the important contributions in semiempirical chemical shift calculation routines (*39*).

Nevertheless, despite its apparent similarity with the above described situation, the situation of resion bound peptides is fundamentally different. Indeed, the analogy with the aromatic ring in a protein stops when we consider the quasi-rigid nature of the protein, resulting in a fixed geometrical relationship between the proton and the aromatic ring. In a resin, the peptide moiety moves with respect to the polystyrene backbone, and this on the very same time scale that was deduced from the NOE enhancement factor. Describing the fluctuations of a magnetic field that experiences a given proton as a simple phenomenon of chemical exchange (*40*), the nanosecond time scale of the movements would make this term very small ($<$1 Hz even for a 10-ppm chemical shift variation at 14 T). We can thus ascribe a unique average chemical shift value to every nucleus, corresponding to its average value over the solid angle that it samples on a very rapid time scale. For equivalent nuclei on different peptides, this value might be slightly different because of random variations in the highly aromatic environment, and this difference will not be averaged out by magic angle spinning. However, in this case of inhomogeneous line broadening (*41*), the individual spin packages (the *spin isochromats*) should be readily refocused by a simple π-pulse in a spin echo experiment and even more so by a train of π-pulses. Our observation that the separation between the π-pulses does influence sizably the measured T_2 times argues against this simple picture of static inhomogeneous broadening.

5. *Slow resin dynamics.* We believe it is possible to reconcile the solution-like properties of the peptides and the anisotropy of the polystyrene backbone in one coherent picture

if we take into account both the anchoring of the peptide and the dynamics of the resin itself. A nucleus on a particular peptide chain that has free rotational diffusion but is still tethered to the backbone will sample on a rapid time scale some part of the complete solid angle, characterized by a well-defined distribution of dipolar fields. Because this movement is on a nanosecond time scale, it will not appreciably contribute to the linewidth. However, whereas the resin itself is immobile on this nanosecond time scale, its slower movements will be at the origin of a variable averaged dipolar field in the region that the proton can sample. Residual dipolar interactions with correlation times superior to 10^{-4} s were concluded from the observed super-Lorentzian lineshapes of the ^{1}H NMR lines in cross-linked polystyrene resins swollen in $CDCl_3$ under nonspinning conditions (*42*). Variations corresponding to as little as 60 Hz (0.1 ppm in proton frequency, or 1 ppm for the nitrogen) in the averaged dipolar field experienced by a given peptide chain over its accessible volume will lead to a broadening on the order of several hertz, if these changes occur at the millisecond time scale, which brings us into the regime of intermediate to fast exchange. These fluctuations can hence explain the differences in linewidth that we observe for resin bound and free peptides.

Experimental evidence for this scenario that takes into account both the rapid peptide movement and the slower resin dynamics was obtained through T_2 measurements with different delays separating the π-pulse in the CPMG train (Table 1). Indeed, the obtained T_2 values clearly increase upon decreasing the value of δ, and for the smallest value, $\delta = 83\ \mu$s, the T_2 times for the two N terminal residues approach the theoretical value of 400–500 ms based on the correlation time τ_c and the classical expression of T_2 relaxation from dipolar and CSA based mechanisms. Whereas the proton longitudinal relaxation could possibly contribute to the T_2 relaxation in the case of the longer δ delays because of the formation of antiphase H_zN_x magnetization terms, this effect is too small to explain the decrease in transverse relaxation rates observed upon shortening the δ delays (*42*). For the Gly residue, a similar trend of increasing T_2 times with decreasing δ intervals was observed, but the limiting value of 184 ms observed still falls short of the theoretical 444 ms.

A theoretical expression has been derived for the observed T_2 relaxation rate in a CPMG experiment in the case of two-site exchange (*25*). In our case, however, a distribution of average chemical shift values is expected, but the absence of information on its amplitude, its population levels, and the time scale of the exchange makes an analytical description beyond reach. Still, for the case of two-site exchange it was shown that when the delay δ is short compared to the time constant that characterizes the exchange, the effects of chemical exchange are continuously refocused and hence attenuated. Moreover, in this model, the δ delay that leads to a T_2 value halfway between its extreme values corresponding to a fully effective and a fully refocused chemical exchange process roughly corresponds to the characteristic exchange time scale. For the Ala residue, we can fit the experimental results nicely to this model, if we assume

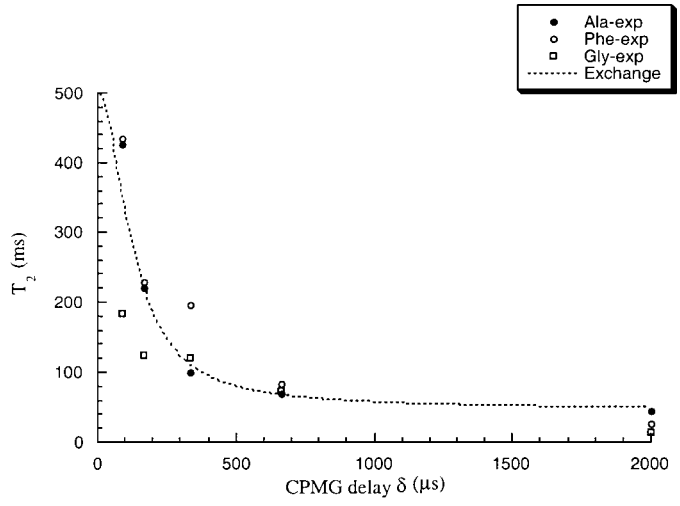

FIG. 4. Graphical representation of the relaxation data of Table 1. The curve represents the best fit through the relaxation data of the Ala ammonium nitrogen (solid circles), as calculated with the formula given in Methods, with $(500\ \mu s)^{-1}$ for k_{exch}, 90 Hz for $\Delta\omega/2\pi$, and a dipolar relaxation rate of 500 ms. The data for the Gly amide nitrogen are given by empty squares, whereas those for Phe are indicated by empty circles.

values of $(500\ \mu s)^{-1}$ for k_{exch} and 90 Hz for $\Delta\omega/2\pi$ (Fig. 4). Whereas these values compare well with those derived from the super-Lorentzian lineshapes (*43*), the situation seems more complicated for the Gly residue, where we see a static inhomogeneous contribution that is refocused by a train of π-pulses even when they are separated by the longest delay of 667 μs, but where simultaneously a rapid exchange process is active that cannot even be refocused by the CPMG pulses when they are separated by 83 μs. Because this residue is juxtaposing the resin, we can indeed imagine that it is subject to an increased spatial restriction leading to distinguishable spin isochromats, at least on a millisecond time scale, which explains the immediate increase of the apparent relaxation rate when we refocus this through π-pulses. On the other hand, this same parameter of enhanced local restriction will make it particularly sensitive to the movements of individual aromatic rings, and especially that ring through which it is linked to the polystyrene backbone. The Ala nitrogen nucleus sees a more averaged picture because of its larger distance from the resin implying greater freedom of motion. The Phe residue is somehow between both these extremes, with some residual static inhomogeneous broadening but less than for the grafted Gly and with a rapid time component that is still slower than for the Gly nitrogen, because it is basically refocused when using δ values of 83 μs. Interpretation of the data for the Phe residue are moreover hampered by the aromatic nature of its side chain, which potentially might undergo hindered rotation.

It is clear that our analysis is at most qualitative, even though it leads to reasonable estimates for both $\Delta\omega$ and k_{exch} in the case of the Ala residue. However, the important factor is that for all three nitrogens considered, the T_2 times increase upon

decreasing δ values. This clearly indicates that a slow process is responsible at least in part for the observed line broadening, and, in agreement with previous analysis of the proton lineshape, we identify it here as the dynamics of the resin. Future investigations of resins with variable degrees of cross-linking will be of further interest to firmly establish our hypothesis.

Whereas numerous studies in the past have used spectroscopic techniques such as electron paramagnetic resonance (EPR) or NMR to probe the mobility of the pendant groups on the resin (for a review, see (*28*)), our present results indicate an observation that directly relates to the mobility of the polymer backbone, and this below the glass transition temperature T_g at which substantial motion of the polymer begins. Moreover, contrary to EPR studies where the concentration of free radicals has to be kept low in order to avoid large spin–spin couplings or Heisenberg exchange terms (*44*), NMR has no such limitations, and the full loading can be used. A major advantage of this fact is a diminished risk for the probe going only into the more accessible regions that mostly correspond to the lesser degree of cross-linking. A very interesting corollary of our results therefore might be the possibility of observing multiexponential relaxation indicating a heterogeneity of the resin dynamics due to a heterogeneity in cross-linking in the individual beads, although the fitting of multiexponential curves can pose severe numerical problems when the time constants are not very different. The LCC dynospheres are described to show a homogeneous cross-linking throughout the bead (*45*). In agreement with this, we obtained a good exponential fit for the decaying transverse magnetization component at all δ delays (Fig. 3), indicating a homogeneous behavior of the resin contribution to the transverse relaxation rates. Further efforts will go to look to the same behavior in differently cross-linked resins to estimate how resin cross-linking affects the resin contribution to the linewidth. Working with mixture of differently cross-linked beads should further allow us to assess the signal-to-noise ratio and other related NMR parameters to detect multiexponential relaxation. Finally, this could provide for the first time an analytical means to monitor the homogeneity of the cross-linking of a solid phase resin sample.

ACKNOWLEDGMENTS

We thank Professor D. Live for sharing literature of earlier NMR measurements on solid phase resins. G.C. acknowledges Hoechst Marion Roussel (Romainville) for a post-doctoral fellowship. We thank Dr. W. Glettig (LCC, Switzerland) for a generous gift of the dynospheres and for many insightful discussions. The 600-MHz facility used in these studies was funded by the Région Nord-Pas de Calais (France), the CNRS, and the Institut Pasteur de Lille.

REFERENCES

1. W. L. Fitch, G. Detre, C. P. Holmes, J. N. Shoorely, and P. A. Keifer, *J. Org. Chem.* **59,** 7955 (1994).
2. R. C. Anderson, J. P. Stokes, and M. J. Shapiro, *Tetrahedron Lett.* **36,** 5311 (1995).
3. R. C. Anderson, M. A. Jarema, M. J. Shapiro, J. P. Stokes, and M. J. Zilix, *J. Org. Chem.* **60,** 2650 (1995).
4. P. A. Keifer, *J. Org. Chem.* **61,** 1558 (1996).
5. I. Pop, C. Dhalluin, B. Depréz, P. Melnyk, G. Lippens, and A. Tartar, *Tetrahedron* **52,** 12209–12222 (1996).
6. C. Dhalluin, I. Pop, B. Depréz, P. Melnyk, A. Tartar, and G. Lippens, *in* "ACS Symposium Series: Molecular Diversity and Combinatorial Chemistry" (I. M. Chaiken and K. D. Janda, Eds.), American Chemical Society, Washington DC (1996).
7. M. Grotli, C. H. Gotfredsen, J. Rademann, J. Buchardt, A. J. Clark, J. O. Duus, and M. Meldal, *J. Comb. Chem.* **2,** 108–119 (2000).
8. J. Furrer, M. Piotto, M. Bourdonneau, G. Guichard, D. Limal, K. Elbayed, J. Raya, J.-P. Briand, and A. Bianco, *J. Am. Chem. Soc.* **123,** 4130–4138 (2001).
9. A. Bianco, J. Furrer, D. Limal, G. Guichard, M. Piotto, J. Raya, K. Elbayed, and J.-P. Briand, *J. Comb. Chem.* **6,** 681–690 (2000).
10. H. Y. Carr and E. M. Purcell, *Phys. Rev.* **94,** 630–638 (1954).
11. S. Meiboom and D. Gill, *Rev. Sci. Instrum.* **29,** 688–691 (1958).
12. M. Delepierre, A. Prochnika-Chalufour, J. Boisbouvier, and L. D. Possani, *Biochemistry* **38,** 16756 (1999).
13. M. Piotto, M. Bourdonneau, J. Furrer, A. Bianco, J. Raya, and K. Elbayed, *J. Magn. Reson.* **149,** 114 (2001).
14. J.-M. Wieruszeski, G. Montagne, G. Chessari, P. Rousselot-Pailley, and G. Lippens, *J. Magn. Res.* **152,** 95–102 (2001).
15. L. E. Kay, L. K. Nicholson, F. Delaglio, A. Bax, and D. A. Torchia, *J. Magn. Reson.* **97,** 359–375 (1992).
16. J. Cavanagh, W. J. Fairbrother, A. G. Palmer III, and N. J. Skelton, "Protein NMR Spectroscopy: Principles and Practice," Academic Press, San Diego, 1996.
17. Y. Hiyama, C. H. Niu, J. V. Silverton, A. Bavoso, and D. A. Torchia, *J. Am. Chem. Soc.* **110,** 2378–2383 (1988).
18. G. Chessari, J.-M. Wieruszeski, and G. Lippens, *J. Am. Chem. Soc.* **123,** 12103–12104 (2001).
19. A. Abragam, "The Principles of Magnetic Resonance," Clarendon Press, Oxford, UK (1961).
20. N. R. Nirmala and G. Wagner, *J. Am. Chem. Soc.* **110,** 7557–7558 (1988).
21. J. Peng and G. Wagner, *J. Magn. Reson*. **98,** 308–332 (1992).
22. C. Dhalluin, C. Boutillon, A. Tartar, and G. Lippens, *J. Am. Chem. Soc*. **119,** 10494–10500 (1997).
23. G. Lippens, M. Bourdonneau, C. Dhalluin, R. Warrass, T. Richert, C. Seetharaman, C. Boutillon, and M. Piotto, *Current Org. Chem.* **3,** 147–169 (1999).
24. G. M. Clore, P. C. Driscoll, P. T. Wingfield, and A. M. Gronenborn, *Biochemistry* **29,** 7387–7401 (1990).
25. M. Bloom, L. W. Reeves, and E. J. Wells, *J. Chem. Phys.* **42,** 1615–1624 (1965).
26. Y. Yu, V. Y. Orekhov, K. V. Pervushin, and A. S. Arseniev, *Eur. J. Biochem.* **219,** 887–896 (1994).
27. G. Lippens, J.-M. Wieruszeski, D. Horvath, P. Talaga, and J.-P. Bohin, *J. Am. Chem. Soc.* **120,** 170–177 (1998).
28. A. R. Vaino and K. D. Janda, *J. Comb. Chem.* **2,** 579–596 (2000).
29. For a review, see A. G. Palmer III, J. Williams, and A. McDermott, *J. Phys. Rev.* **100,** 13293–13310 (1996), and references therein.
30. D. Live and D. S. B. H. Kent, *in* "Elastomers and Rubber Elasticity," ACS Symposium Series, Vol. 193, pp. 501–515, Amer. Chem. Soc., Washington DC (1982).
31. E. Bayer, K. Albert, H. Willisch, W. Rapp, and B. Hemmassi, *Macromolecules* **23,** 1937–1940 (1990).

32. K. Elbayed, M. Bourdonneau, J. Furrer, T. Richert, J. Raya, J. Hirschinger, and M. Piotto, *J. Magn. Res.* **136,** 127–129 (1999).

33. D. L. Vanderhart, W. L. Earl, and A. N. Garroway, *J. Magn. Reson.* **44,** 361–401 (1981).

34. K. Wüthrich, *in* "NMR of Protein and Nucleic Acids," Wiley-Interscience, New York (1986).

35. J. A. Pople, *J. Chem. Phys.* **24,** 1111–1116 (1956).

36. H. M. J. McConnell, *J. Chem. Phys.* **27,** 226–229 (1957).

37. D. L. Vanderhart, *in* "Encyclopedia of Nuclear Magnetic Resonance" (D. M. Grant and R. K. Harris, Eds.), Vol. 5, pp. 2938–2946, John Wiley & Sons, West Sussex, UK (1996).

38. G. Lippens and J. Jeener, *Concepts Magn. Reson.* **13,** 8–18 (2001).

39. M. P. Williamson, T. Asalura, E. Nakamura, and M. Demura, *J. Biomol. NMR* **2,** 83–98 (1992).

40. J. I. Kaplan, *in* "Encyclopedia in Nuclear Magnetic Resonance" (D. M. Grant and R. K. Harris, Eds.), Vol. 2, p. 1252, John Wiley & Sons, West Sussex, UK (1996).

41. A. M. Portis, *Phys. Rev.* **91,** 1971 (1953).

42. A. G. Palmer III, N. J. Skelton, W. J. Chazin, P. E. Wright, and M. Rance, *J. Magn. Reson.* **75,** 699–711 (1992).

43. D. Doskocilova, B. Schnieder, and J. Jakes, *J. Magn. Reson.* **29,** 79–90 (1978).

44. M. E. Wilson, J. A. Wilson, and M. J. Kurth, *Macromolecules* **30,** 3340 (1997).

45. See the LCC Web site http://www.chemsupply.ch.